IOSR Journal of Mechanical and Civil Engineering (IOSR-JMCE)
e-ISSN: 2278-1684,p-ISSN: 2320-334X, Volume 19, Issue 5 Ser. I (Sep. – Oct. 2022), PP 39-49
www.iosrjournals.org

Structural Behavior of Corroded Beams - Numerical and Analytical Approach

Ahmed. E. Marawan[1*], Ahmed. S. Debaiky[2], Ahmed. H. Abdel-Kareem[2]
[1] *Civil Engineering Department, Delta University, Gamsa, Egypt*
[2] *Civil Engineering Department, Banha University, Banha, Egypt*
[*] *Corresponding author: engamarawan1989@gmail.com*

Abstract
To simulate corrosion deterioration on load carrying capacities, deflection and slip between concrete and steel for R.C. beams, a 3-D F.E. model was considered by using ANSYS software. Several F.E. models were created to simulate different levels of corrosion. In this model, both concrete and steel were modelled as solid elements and stirrups were represented as link elements. To consider corrosion effects which can be represented by reduction in steel cross section and decrease in bond between concrete and steel, contact element between two bodies was created. Also, analytical calculations were driven to calculate load carrying capacities, deflection and slippage distance. The results of both models were acceptable within average error about 10%.

Keywords: *Corrosion; numerical model; analytical calculation; load carrying; deflection; slip.*

Date of Submission: 20-09-2022 Date of Acceptance: 05-10-2022

I. Introduction

The durability problems of reinforced concrete structures have a widelygreat concerning. One of the durability problems is steel corrosion. Steel corrosion negatively influences in deterioration of reinforced structures, especially in corrosive environments. The corrosion phenomenon causes steel mass loss, decreasing the bond strength between concrete and rebars and have a negative impact on behavior of bond-slip relationship between rebars and concrete. Moreover, steel corrosion leads to cracks and cover spalling. All of these parameters have effects on structural behavior of structures. One of the most remarkable factors due to corrosion is mass loss of steel, which consequentlyleads to reduction of rebars cross section.The main types of corrosion which deteriorate the structures are carbonation induced corrosion and chlorides induced corrosion. The carbonate corrosion leads to uniform reduction in steel rebars. On contrary, pitting corrosion happens due to chlorides corrosion [1]. Pitting corrosion is localized with considerable reduction in rebars area, which sometimes formed without any signs [2-4]. Rodriguez et al. [5] created a model to calculate attack penetration from the measured mass loss, where in uniform corrosion the pitting factor was 2, whilst in pitting corrosion the pitting factor was taken from 4 to 8[6].

For An adequate representation of corrosion, bond deterioration between rebars and concrete and also, a reduction of steel bars must be fully discussed. Many researchers developed analytical models and numerical simulationsand validated their models with pervious experimental studies. Huang and Yang [7] proposed an analytical model to predict load carrying capacity of corroded members according to their corrosion rate. El-Maaddawy et al. [8] created model to predict the flexural capacity of corroded R.C. beams with sustained loads and without any loads. Their model can predict load-deflection curves by calculating elongation of steel bars between concrete mean crack spacing. Simplified model was conducted by Wang and Liu [9]to investigate the residual strength of corroded doubly R.C. beams. Besides, artificial neural network was proposed by Imam et al. [10] to predict the strength of corroded R.C. members. In addition to, Ahmed [11] proposed an empirical model to predict the residual flexural strength of corroded R.C. beams. This model which was conducted depending on current density and duration for corrosion and steel bar diameter.

In addition to analytical model, F.E. models were used to simulate the influence of corrosion. Berra et al. [12] investigated the deterioration of bond strength between concrete and rebars due to corrosion products. The simulation was conducted by ABAQUS. Xiaoming and Hongqiang [13] conducted a study on R.C. beams which were subjected to low levels of corrosion. The analysis was performed by F.E. software ANSYS. They concluded that when corrosion rate was 4% to 7% there was a decrease in loading capacity. Furthermore, Ghods et al. [14] prepared F.E. model by using ANSYS software. The model takes into account the reduction of rebars area and the change in bond strength between concrete and rebars. When the ANSYS results were compared to

the experimental data, it was observed that, with an increase of corrosion rate, the load carrying capacity and bond strength of beams were decreased.

II. Objectives

One of the objectives of this study iscreating 3-D model by using ANSYS software to represent corrosion of R.C. beams. Moreover, an analytical model was developed. The results obtained from the two models were compared with the available experimental data. Finally, load carrying capacity, deflection and slippage distance were the parameters to verify the models.

III. Flexural corroded R.C. beams: Numerical and Analytical model

3-1 Experimental case study

To predict the structural behavior of corroded R.C. beams numerically and analytically, an extended study was done on experimental results for corroded beams that had done by Marawan et al. [15]. Propreties of materials, current density of corrosion and mass loss of steel bars for each beam were clearly reported. In addition, geometry of beams, rebars details and loading boundary were clearly illustrated as shown in Fig. (1).

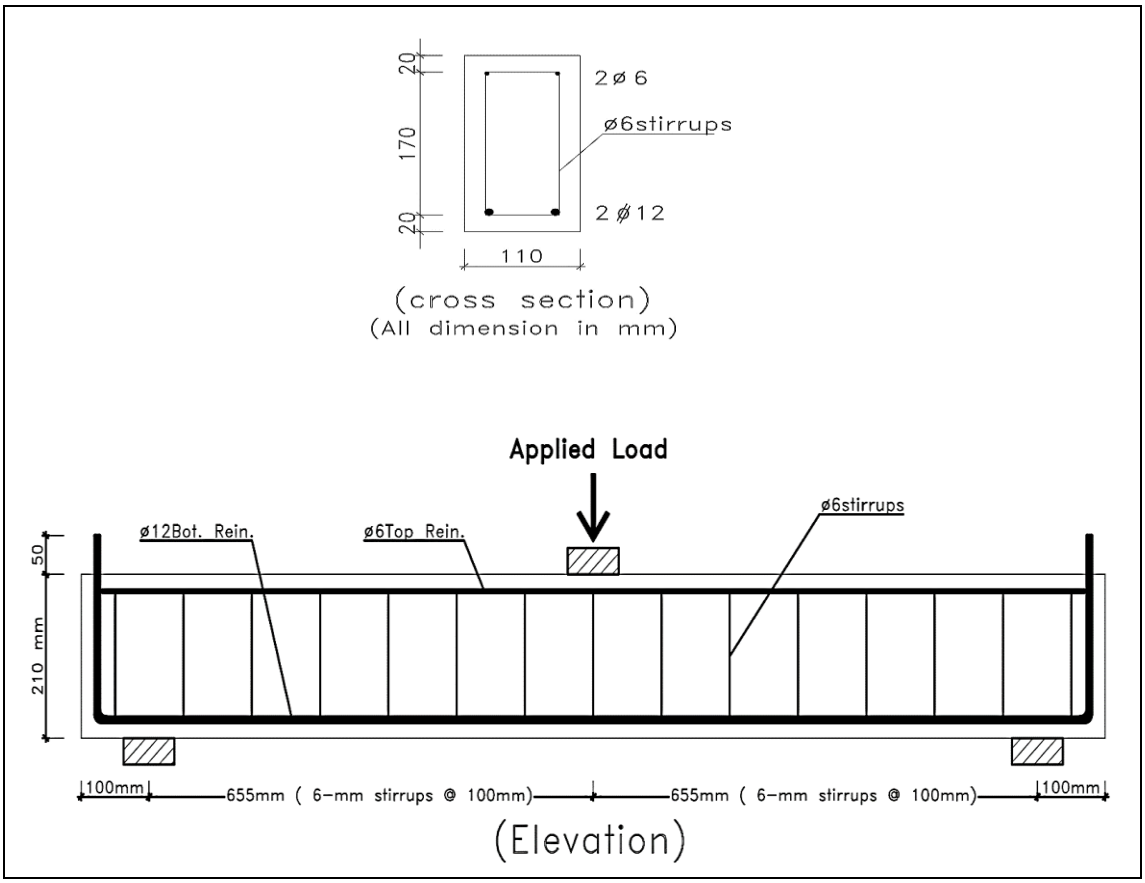

Fig. (1): Details of specimens

3-2 Numerical modelling

For the simulation of corroded R.C. beams, student finite element software ANSYS 2021 R2 version was used for developing finite element model. F.E model was utilized to investigate 8-R.C. corroded beams with variable corrosion rate and compressive strength as shown in Table (1). Finally, the model results were verified with experimental results.

Table (1): Compressive strength and corrosion rate of R.C. beams

Specimens	Compressive strength f_c (MPa)	Steel mass loss (%)
B1	44.6	6.7
B2		6

B3	44.3	5.1
B4		4.9
B5	49.4	4.6
B6		3.8
B7	40	4.7
B8		5

3-2-1Concrete element and properties

Solid 185 element was used to model concrete. Solid 185 is 3-D element with 8-nodes as shown in Fig. (2). At each node, there are 3-translational degrees of freedom in nodal direction. Furthermore, Solid 185 has the ability to hyper-elasticity, plastic deformation, stress stiffening, large strain and large deformation.

For concrete properties, elastic-plastic constitutive model, according to Druker-Prager failure condition, was applied as shown in Fig. (3). Uniaxial compressive stress, uniaxial tensile stress, biaxial compressive stress, modulus of elasticity and Poisson's ratio values were all defined to model concrete properties as shown in Table (2).

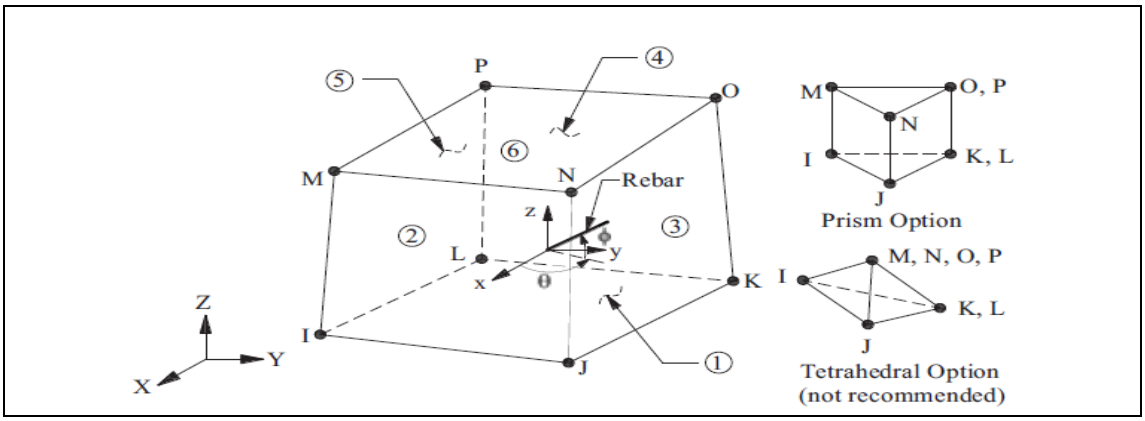

Fig. (2): Solid 185 element geometry

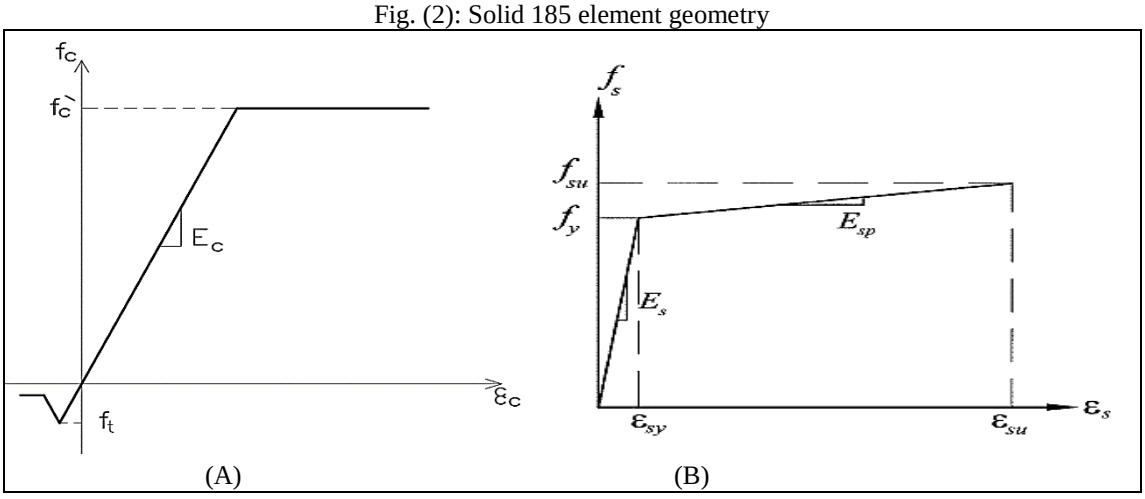

Fig. (3): Material modeling: (A) Concrete; (B) Steel

Table (2): Concrete properties for solid 185 (B1 and B2)

property	Value
Modulus of elasticity	31400 MPa
Poisson's ratio	.2
Druker-Prager criteria	
Uniaxial compressive stress	44.6 MPa
Uniaxial tensile stress	4.5 MPa

Biaxial compressive stress	50 MPa

3-2-2 Steel element and properties

For top and bottom steel reinforcing bars, solid 45 was adopted, wherein Solid 45 element is a 3-D element with 8-nodes as shown in Fig. (4). At each node, there are 3-translational degrees of freedom in nodal direction. Solid 45 has the ability to hyper-elasticity, plastic deformation, stress stiffening, large strain and large deformation.

For stirrups, link 180 element was considered. This element has a capability of carrying compression and tension stresses. Link 180 element has 2-node with 3 degrees of freedom at each node as shown Fig. (4).

Table (3) illustrates the steel properties of each rebars and stirrups. Steel bars were supposed to be as a complete elastic-plastic body and constitutive model considered on Von Mises failure condition was utilized. As shown in Fig. (3), stress-strain curve of steel is assumed to be linear elastic-plastic with 1% postyield hardening.

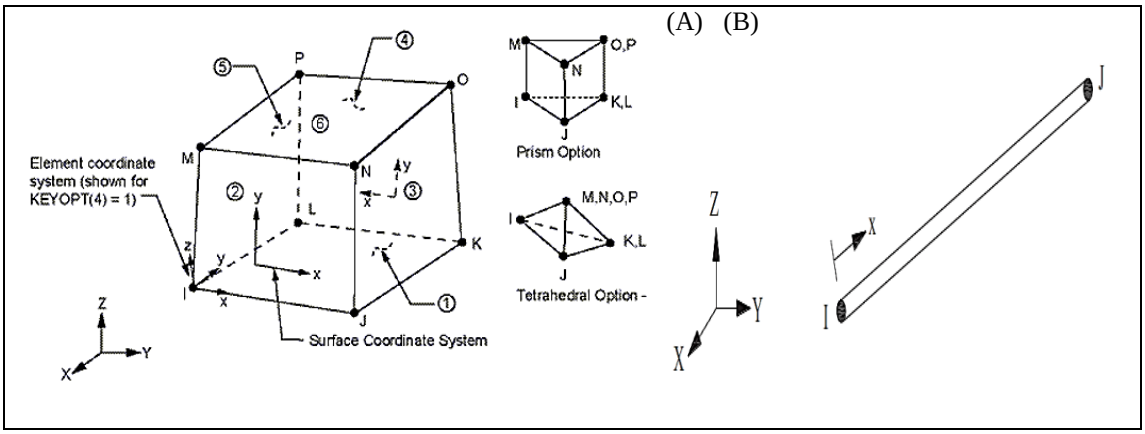

Fig. (4): Element geometry: (A): Solid 45; (B): Link 180

Table (3): steel properties for solid 45 and link 180

property	Value
Modulus of elasticity	2*105 MPa
Poisson's ratio	.3
bilinear criteria	
Yield stress for Ø 12 mm	617 MPa
Yield stress for Ø 6 mm	315 MPa
Tangent modulus	2000 MPa

3-2-3 Bonding element

Contact element is provided by F.E.M analysis to account the interface between concrete and steel. The contact element is a conventional method when modelling two separated bodies. The contact element consists of two surfaces; the first surface is the contact surface (CONTA 174) which was adjacent to steel and the other surface is the target surface (TARGE 170) which was connected to concrete. To use contact element to represent corrosion layer, contact stiffness (Kcont) was adjusted by determining normal contact stiffness factor (FKN), tangent contact stiffness factor (FKT) and penetration tolerance (FTOLN).As for ANSYS software, it uses variable bond models wherein each model has different properties that change contact surface behavior. In this study,the established bond model was "bonded contact behavior". Also, the used algorithm in this study was penalty where there are three main contact algorithms. And then, penetration depth, slippage distance, steel stress and load carrying capacity of beam were all observed to evaluate the effective contact element.

3-2-4 Creating model

Fully scale reinforced concrete beams were modelled by ANSYS workbench which provides much easier tools for modelling. To model existing beam, concrete cross section was created in X-Y plan and then extruded in orthogonal direction. To present top and bottom steel bars as solid bodies, the rebars location was

cut off from concrete body and then steel bars cross sections were created and extruded in longitudinal direction of beam. Finally, stirrups were considered as line element and replicated along longitudinal axis as shown in Fig. (5). Due to technique of modelling concrete and rebars as solid bodies, contact element was created automatically. By creating contact element, corrosion effects were considered. For modelling supports, bottom edge on X-direction at one end of beam was constrained in all direction (X, Y and Z) and other end of beam was constrained in directions (X and Y). loading condition was applied by assigning 15 mm vertical displacement at the middle of top surface of beam according to the average vertical deflection on experimental works. To attain an accurate solution, all elements were divided to small elements with using F.E. mesh command as shown in Fig. (6).

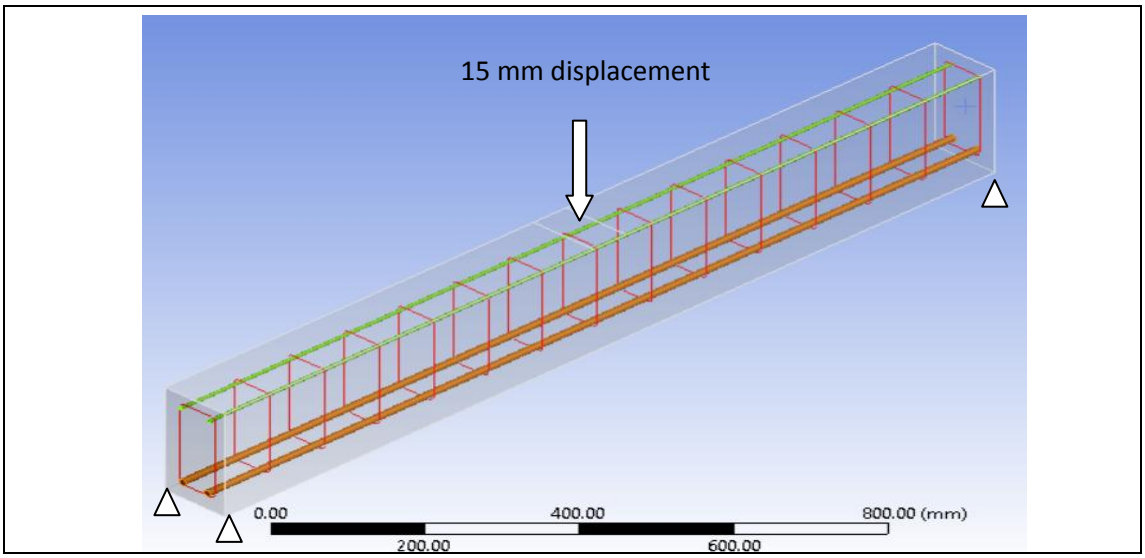

Fig. (5): Modelling of beam

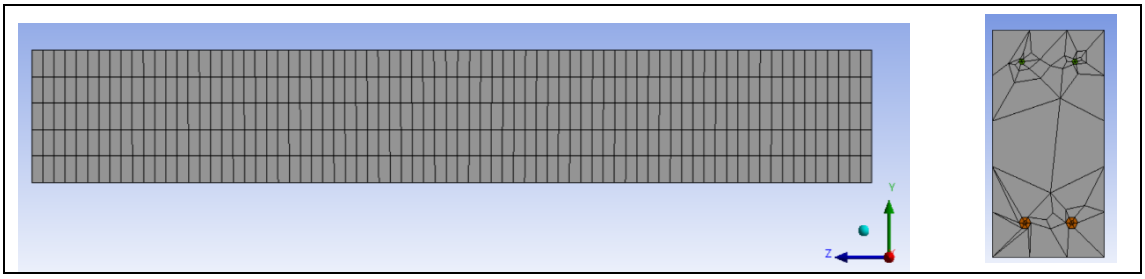

Fig. (6): Meshing of beam

3-3Analytical modelling

To verify the experimental and numerical results with analytical result, analytical model was used to predict the flexural behavior of corroded beams. The model takes into account the formation of rust layer which changes the bond strength between concrete and steel and also, reduces the steel cross section. This process enables the model to calculate deflection, slippage distance and load carrying capacity.

3-3-1Load bearing capacity

To calculate steel stress at any section of beam, equilibrium and compatibility requirements must be achieved. For equilibrium condition, the sum of axial forcesover the section should be zero and external bending moments should be equal to internal moments. In addition, strain at any point is proportional to its distance from the neutral axis to achieve strain compatibility. As shown in Fig. (7), the stress and strain distribution over the beam section were illustrated.

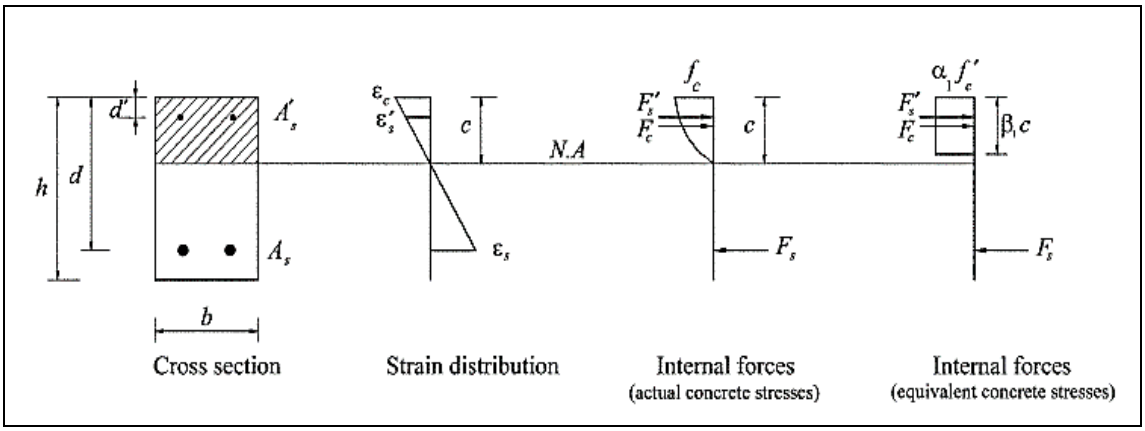

Fig. (7):Stress and strain distribution over section

Eq. (1) toEq. (4) were considered for equilibrium condition in pre-yield and post-yield stages respectively.

$$\alpha_1 \grave{f}_c\, \beta_1\, c\, b + \grave{A}_s E_s \frac{\varepsilon_c\,(c - \grave{d})}{c} = E_c\, b\, \frac{\varepsilon_c\,(h-c)^2}{2c} + A_s E_s \frac{\varepsilon_c\,(d-c)}{c} \qquad \text{Eq. (1)}$$

$$\alpha_1\, \grave{f}_c\, \beta_1\, c\, b \left(c - \frac{\beta_1\, c}{2}\right) + \grave{A}_s E_s \frac{\varepsilon_c\,(c-\grave{d})^2}{c} + E_c\, b\, \frac{\varepsilon_c\,(h-c)^3}{3c} + A_s E_s \frac{\varepsilon_c\,(d-c)^2}{c} = M_{Ext} \qquad \text{Eq. (2)}$$

$$\alpha_1\, \grave{f}_c\, \beta_1\, c\, b + \grave{A}_s E_s \frac{\varepsilon_c\,(c-\grave{d})}{c} = A_s \left[f_y + E_{sp}\left(\frac{\varepsilon_c\,(d-c)}{c} - \frac{f_y}{E_s}\right)\right] \qquad \text{Eq. (3)}$$

$$\alpha_1\, \grave{f}_c\, \beta_1\, c\, b \left(c - \frac{\beta_1\, c}{2}\right) + \grave{A}_s E_s \frac{\varepsilon_c\,(c-\grave{d})^2}{c} + A_s\,(d-c)\left[f_y + E_{sp}\left(\frac{\varepsilon_c\,(d-c)}{c} - \frac{f_y}{E_s}\right)\right] = M_{Ext} \qquad \text{Eq. (4)}$$

3-3-2 Slippage distance

To investigate the slippage distance, the beam was divided into elements. Each element was considered to have one crack at the middle of the element as shown in Fig. (8).

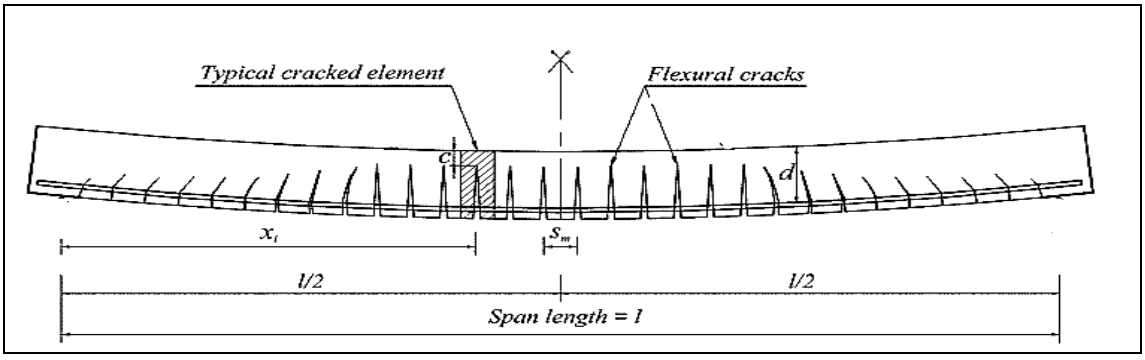

Fig. (8):Modelling of the beam

also, spacing between cracks was considered as constant which can be expressed as

$$s_m = 2(C + \frac{s}{10}) + k_1 k_2 \frac{d_b\, h_{eff}\, b}{A_{st}} \qquad \text{Eq. (5)}$$

$$k_2 = 0.25\, \frac{\varepsilon_1 + \varepsilon_2}{2\varepsilon_1} \qquad \text{Eq. (6)}$$

To account the slippage distance for each element, the relative elongation between concrete and steel (es-ec) was considered. The slippage occurred when the applied load exceeded the cracked load.

Considering Eq. (7) to Eq. (9), element slippage was

$$s_i = \frac{1}{2}\,(e_i - s_m \varepsilon_r) \qquad \text{Eq. (7)}$$

$$e_i = \frac{s_m}{E_s}\left(f_{max} - \frac{\tau_c s_m}{d_b}\right) \quad \text{for preyield stage} \qquad \text{Eq. (8)}$$

$$e_i = \frac{s_m}{E_s}\left(f_y - \frac{\tau_c s_m}{d_b}\right) + \frac{s_m}{E_{sp}}\left(f_{max} - f_y\right) \quad \text{for postyield stage} \quad \text{Eq. (9)}$$

To account the effect of corrosion, bond stress was modified based on fib model code 2010 [15], which was confined with stirrups as given

$$\tau_c = (A_1 + A_2)\, m \left(0.55 + 0.24\frac{c_c}{d_b}\right)\sqrt{f_c} + 0.191\frac{A_t f_{yt}}{s_s d_b} \qquad \text{Eq. (10)}$$

The values of A1 and A2 depend on the used current density for formation corrosion as shown in Table (4).

Table (4): Values of A1 and A2

Current density (μA/cm^2)	A1	A2
40	1.003	-0.037
90	1.104	-0.024
150	1.152	-0.021
250	1.163	-0.011
500	0.953	-0.014
1000	0.861	-0.014
2000	0.677	-0.009
4000	0.551	-0.01

3-3-3 Beam deflection

Deflection of beams was considered from elongation of stabilized cracked elements rather than from curvature of beam. To account the deflection of beam, left-side or right-side elements were considered to calculate the deflection of each element as shown in Fig. (8). Deflection of beam was expressed as

$$\Delta = \sum_{i=1}^{i=n} \frac{e_i}{d-c} \qquad \text{Eq. (11)}$$

IV. Verification against the experimental results

4-1 Loading capacity and deflection

Finite element model and analytical model were carried out for 8-beams with various levels of corrosion. Load carrying capacities, deflection and slippage distance were considered to evaluate the F.E. model and analytical model.

For load carrying capacities and deflection values from experimental, F.E. model and analytical model, Table (2) illustrated acceptable agreement between predicted values and experimental results.

Table (5): Loading capacity and deflection

specimen	Experimental		ANSYS		Analytical	
	Load (KN)	Deflection (mm)	Load (KN)	Deflection (mm)	Load (KN)	Deflection (mm)
B1	74.5	15.9	76.6	15	71.7	12.8
B2	75.6	15.1	78.2	15	72.5	12.7
B3	77.4	19.2	78.1	15	73.2	12.4
B4	78.5	13.3	79.8	15	73.5	12.1
B5	84.3	15.2	84.2	15	74.6	12.8
B6	86.9	15.7	85.5	15	75.3	12.6
B7	83.1	15.7	81.9	15	72.5	12.3
B8	80.2	14.0	80.8	15	72.1	12.1

From Table (5), it was observed that the accuracy of F.E. model to predict load capacity and deflection of beams was acceptable. The percentage of error to calculate loading capacity was +2.9%, +3.4%, +1%, +1.7%, -.02%, -1.7%, -1.5% and +1% for B1, B2, B3, B4, B5, B6, B7 and B8 respectively. Also, the error of deflection was -5.5%, -1.0%, -21%, +13%, -2%, -4.5%, -4.5% and +7.1% for B1, B2, B3, B4, B5, B6, B7 and B8 respectively.

In addition, the accuracy of analytical model to predict load capacity and deflection of beams was acceptable. The percentage of error to calculate loading capacity was -3.7%, -4.1%, -5.4%, -6.3%, -11.5%, -13.2%, -12.5% and -9.9% for B1, B2, B3, B4, B5, B6, B7 and B8 respectively. Also, the error of deflection

was-19.5%, -15.9%, -33.4%, -9%, -15.7%, -19.5%, -21.1% and -13.6% for B1, B2, B3, B4, B5, B6, B7 and B8 respectively. The percentage of any error was estimated according to the following equation

$$Error\ \% = \frac{(\text{predicted value} - \text{expermental value})}{\text{expermental value}} \text{ x } 100 \qquad \text{Eq. (12)}$$

Fig. (9) and Fig. (10) showed the load-deflection curves for loaded corroded beams and unloaded corroded beams respectively.

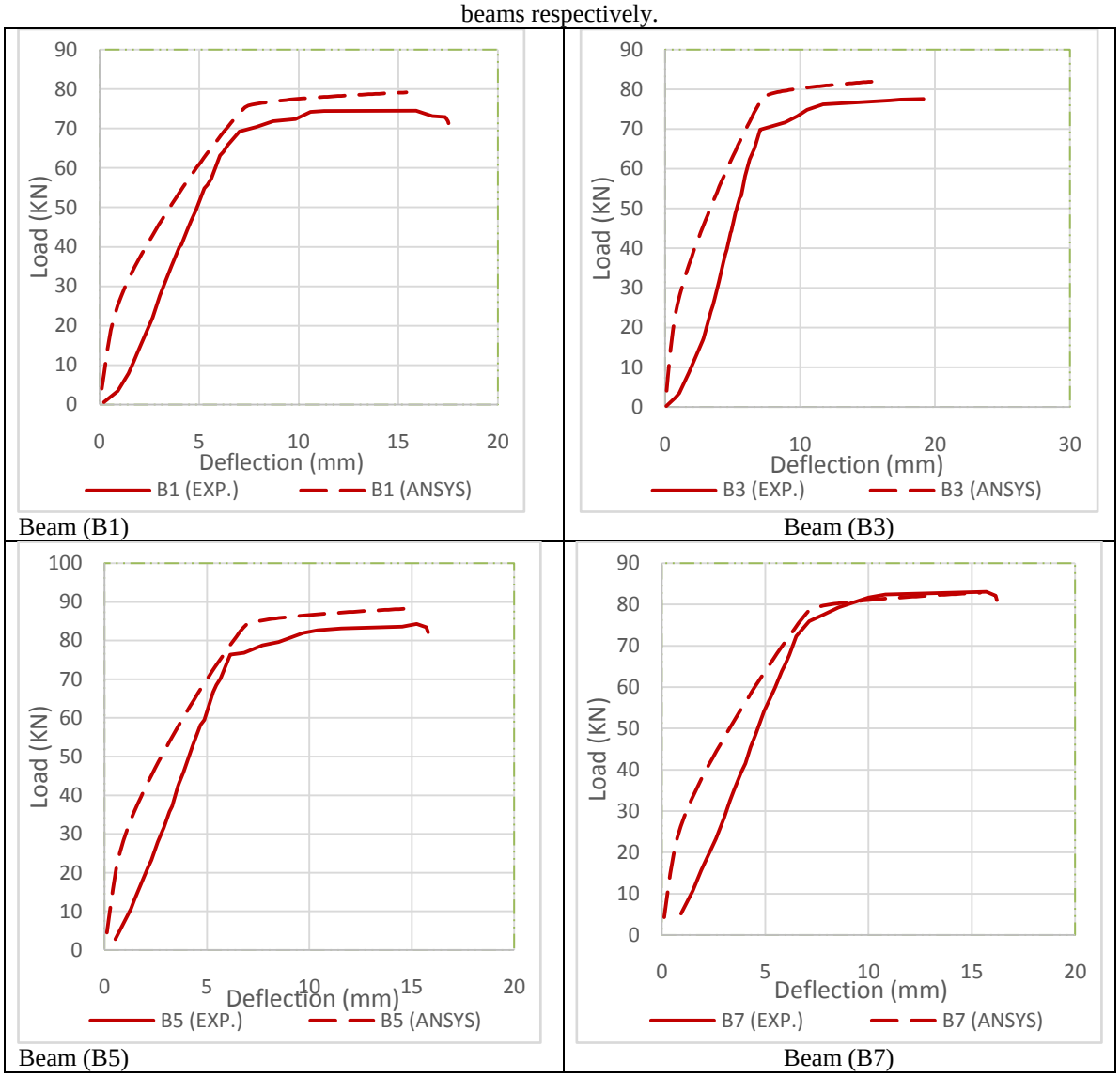

Fig. (9):Load-deflection curves of preloaded corroded beams

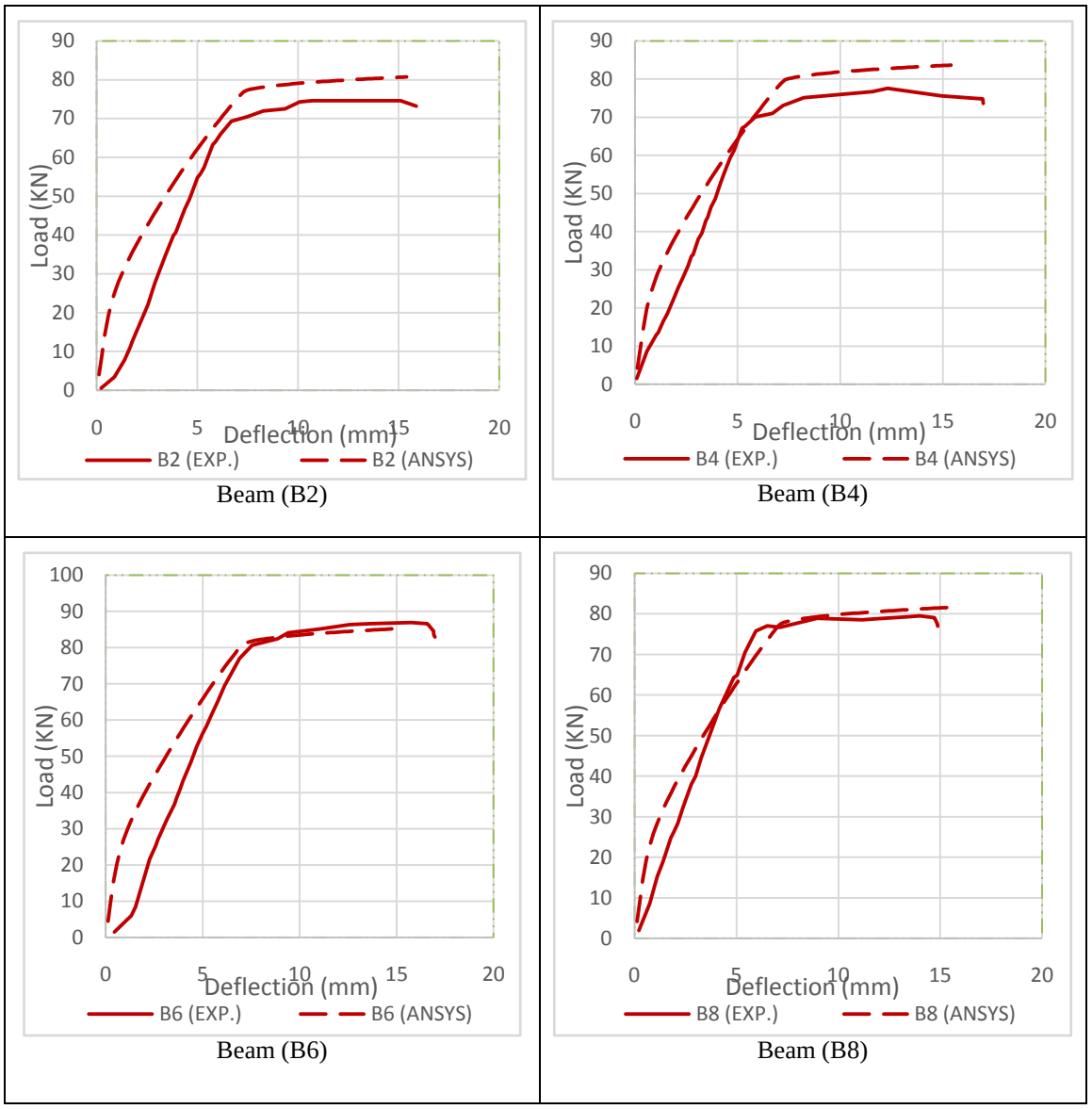

Fig. (10):Load-deflection curves of unloaded corroded beams

4-2 Slippage distance

Finite element model and analytical model had the capability to calculate the slippage distance between concrete and rebars. As shown in Table (6), the values of slip were acceptable. The percentage of error to predict slippage distance was +1%, -1.5%, -10.5%, -3.7%, -14.0%, -14.5%, -6.7% and -7.1% for B1, B2, B3, B4, B5, B6, B7 and B8 respectively. The percentage of slip error was estimated according to the following equation

$$Error\ \% = \frac{(\text{Analytical value} - \text{ANSYS value})}{\text{Analytical value}} \text{ x } 100 \qquad \text{Eq. (13)}$$

Table (6): Slippage distance of beams

specimen	Slip analytical (mm)	Slip ANSYS (mm)
B1	2.47	2.49
B2	2.45	2.42
B3	2.42	2.16
B4	2.42	2.33
B5	2.57	2.21
B6	2.55	2.18
B7	2.24	2.09

B8	2.25	2.09

V. Conclusions

According to analytical and F.E. results which were discussed formerly, a number of conclusions may be considered for the efficiency of models to predict load carrying capacity, deflection and slippage distance of corroded beams. The conclusions are summarized below.

- The ANSYS model can effectively predict the load carrying capacity of corroded beam with considering corrosion effects which negatively influence in cross-section and bond strength between concrete and rebars. The main value of percentages of error in the loading capacity was +7.8% with an average error in deflection equal 1%.
- The uses of contact element between rebars and concrete that were represented as solid element in ANSYS model. By this method, corrosion effects can be simulated.
- ANSYS model showed capability to predict the slippage distance between concrete and steel by change contact between elements. The average percentage of error in predicting slippage was -7.1%.
- Flexural behavior of corroded beans, according to loads-deflection curves which were obtained from ANSYS model,showed acceptable agreement of experimental results.
- Load capacities and deflection of beams which obtained from analytical model showed acceptable agreement of experimental results. The main value of percentages of error in the loading capacity and deflection were -6.2% and -16.4% respectively.
- The values of the slippage of analytical were compatibility with ANSYS model with variation about 7.1%. this acceptable evidence of accuracy of prediction models.

References

a. Kocijan, M. Jenko, Inhibition of the pitting corrosion of Grey cast Iron using carbonate, Mater. Tehnol., 40 (2006) 1, 3–6.
b. R. Boga, Ý. B. Topçu, M. Öztürk, Effect of Fly-Ash amount and Cement type on the corrosion performance of the steel embedded in concrete, Mater. Tehnol., 46 (2012) 5, 511–518.
[2]. J. Cairns, Consequences of reinforcement corrosion for residual strength of deteriorating concrete structures, Proc. of the First Inter. Conference on Behavior of Damaged Structures, Rio de Janeiro, 1998.
[3]. CEB Task Group 2.5, Bond of Reinforcement in Concrete, State-of the art report, fib Bulletin No. 10, 2000
[4]. J. Rodriguez, L.M. Ortega, J. Casal, J.M. Diez, Corrosion of reinforcement and service life of concrete structures, Durab. Build. Mater. Compon. 7 (1) (1996) 117–126.
[5]. Gonzalez, J.A., Andrade, C., Alonso, C., Feliu, S., "Comparison of rates of generalcorrosion andmaximum pitting penetration on concrete embedded steel reinforcement",Cement and Concrete Research, 25(2), 1995, 257-264.
[6]. Huang, R. and Yang, C.C. 1997. Condition Assessment of RC Beams Relative to Reinforcement Corrosion. Cement and Concrete Composites 19: 131-137.
[7]. El Maaddawy, T., Soudki, K., and Topper, T. 2005. Analytical model to predict nonlinear flexural behaviour of corroded reinforced concrete beams. ACI Structural Journal 102(4): 550-559
[8]. Wang, X. and Liu, X.L. 2010. Simplified Methodology for the Evaluation of the Residual Strength of Corroded Reinforced Concrete Beams. Journal of Performance of Constructed Facilities 24(2): 108-119.
[9]. Imam, A., Anifowose, F. and Azad, A.K. 2015. Residual strength of corroded reinforced concrete beams using an adaptive model based on ANN. International Journal of Concrete Structures and Materials 9(2): 159-172.
[10]. Ahmad, S. 2017. Prediction of residual flexural strength of corroded reinforced concrete beams. Anti-Corrosion Methods and Materials 64(1): 69-74
[11]. M. Berra, A. Castellani, D. Coronelli, S. Zanni, G. Zhang, Steel-concrete bond deterioration due to corrosion: finite-element analysis for different confinement levels, Magazine of Concrete Research, 55 (2003) 3, 237 – 247.
[12]. Xiaoming, Y., and Hongqian, Z. (2012). "Finite Element Investigation on Load Carrying Capacity of Corroded RC Beam Based on Bond-Slip." Jordan Journal of Civil Engineering, 6(1), 134-146.
[13]. Ghods, Ali & Sohrabi, Mohammad & Miri, Mahmoud. (2014). Effect of rebar corrosion on the behavior of a reinforced concrete beam using modeling and experimental results. Materiali in Tehnologije. 48. 395-402.
[14]. Ahmed, Marawan & Ahmed, Debaiky & Ahmed, Abdel-Kareem. (2022). Effect of Preloading and Nano-Silica on Structural Behavior of Corroded R.C. Beams. In press
[15]. Fib. Fib Model Code for Concrete Structures 2010; Ernst & Sohn. Wiley: Berlin, Germany, 2013.
[16]. Canadian Standard Associations. S474 concrete structures. Mississauga, Ontario, Canada: Canadian Standard Associations; 2004.

Notation

A_1 and A_2: variables that depend on current density level
A_s: area of tensile steel reinforcement
$À_s$: area of compression steel reinforcement
A_t: cross-sectional area of stirrup
b: width of concrete section
C: clear concrete cover
c: depth of neutral axis of element i measured from top faceof beam
c_c: smaller of concrete clear cover and one-half bar spacing
d: depth of tensile steel reinforcement measured from topface of beam
d′: depth of compression steelreinforcement measured fromtop face of beam

d_b: diameter of tensile steel reinforcing bar
E_c : Young's modulus of concrete
E_s : modulus of steel reinforcement before yielding (pre-yieldstage)
E_{sp} : modulus of steel reinforcement after yielding (post-yieldstage)
e_i: elongation of steel reinforcement between ends of element i
f_c: concrete compressive stress atextreme top fiber of beam
$\grave{f}_c$: concrete compressive strength
f_y: steel yield strength
f_{yt}: yield strength of stirrups
h: height of concrete cross section
h_{eff} :effective embedment thickness
l: span of beam
M_{ext}: external bending moment due to applied loads
m: percent steel mass loss caused by corrosion
n: number of elements within half of beam span
s: spacing between longitudinal steel reinforcing bars
s_i: slip between steel and concrete within element i
s_m: mean crack spacing
s_s: spacing between stirrups
x_i: distance between support and center of element i
α_1 and β_1: stress block factors
Δ: beam midspan deflection
ε_1: concrete strain at bottom of effective embedment zone
ε_2: concrete strain at top of effective embedment zone
$\varepsilon_{c:}$ concrete strain at extreme top fiber of beam
ε_r: concrete cracking strain
κ_1: coefficient that characterizes bond properties at steel-toconcreteinterface
κ_2: coefficient that accounts for strain gradient withineffective embedment zone of concrete
τ_c: bond stress at steel-to-concrete interface

Ahmed. E. Marawan, et. al. "Structural Behavior of Corroded Beams - Numerical and Analytical Approach". *IOSR Journal of Mechanical and Civil Engineering (IOSR-JMCE)*, 19(5), 2022, pp. 39-49.